Vol. 22, n.° 2, julio-diciembre de 2024
ISSN impreso: 1657-6527 • ISSN en línea: 2145-8502

FUENTES
EL REVENTÓN ENERGÉTICO

CHARACTERIZATION AND CO_2 STORAGE CAPACITY ANALYSIS OF THE "LU" RESERVOIR IN THE ORIENTE BASIN

CARACTERIZACIÓN DE LA ARENISCA "LU" Y ANÁLISIS DE SU CAPACIDAD DE ALMACENAMIENTO DE CO_2 EN LA CUENCA ORIENTE

Diego Ayala[1*], Ángel Taday[2], Luis Rivero[1], José Cóndor[3], Jearson Apaza[4]

[1]Departamento de Mineralogía, Petrología y Geología Aplicada, Universidad de Barcelona. Barcelona, España.
[2]Chuanqing Drilling Engineering Company Limited (CCDC). Quito, Ecuador.
[3]Escuela Superior Politécnica del Litoral (ESPOL). Guayaquil, Ecuador.
[4]Reservoir Solution. La Paz, Bolivia.

[*]E-mail: diego.ayala.t@gmail.com

Recibido: 28 de mayo de 2024. Aprobado: 12 de noviembre de 2024. Versión final: 24 de noviembre de 2024.

ABSTRACT

The objective of this work is to determine the CO_2 storage capacity of the Lower "U" reservoir and identify a sealing formation that does not compromise the integrity of the PRH field in the Oriente Basin.

Information obtained from drilled wells in the field, such as core analyses, logs, thin sections analyses, and pressure-transient analyses, were utilized to evaluate the petrophysical properties, the reservoir quality, and the reservoir fluids. Also, petrophysical properties were determined by different methods to address the uncertainty in the measurements. All these properties were utilized in the static and dynamic model to understand the behavior of the Lower "U" reservoir under CO_2 injection as a mechanism to increase the recovery factor (i.e., enhanced oil recovery (EOR) through CO_2 injection). The continuity and adequate CO_2 storage capacity of the Lower "U" reservoir were demonstrated. The presence of a sealing formation of ultra-low permeability/porosity (shale, limestone) above the Lower "U" reservoir provides a safe geological storage system for greenhouse gases (GHG). The central area of PRH field has the best characteristics for CO_2 injection due to low reservoir pressures. Additionally, the azimuth providing greater stability for the CO_2 injection process was determined, preventing the generation of micro-fractures in the Lower "U" and the communication of the sandstone with other formations.

The study incorporated existing information from the oil exploration of the PRH field, and various methodologies were applied to determine petrophysical parameters. Characterizing the Lower "U" provided crucial details about the reservoir, fluids, and lithology. The theoretical storage volume for the Lower "U" reservoir was 9.13 million tons of CO_2. This work is one the very first to assess the carbon capture and storage (CCS) in the Oriente Basin to reduce the environmental impact of GHG emissions.

Keywords: CCS; CO_2 storage; Geological storage; Reservoir; Sandstone; Petrophysics.

Cómo citar: Ayala, D., Taday, A., Rivero, L., Cóndor, J., & Apaza, J. Characterization and CO_2 Storage Capacity Analysis of the "LU" Reservoir in the Oriente Basin. *Fuentes, El reventón energético, 22*(2), 35-54. https://doi.org/10.18273/revfue.v22n2-2024003

RESUMEN

El objetivo de este trabajo es determinar la capacidad de almacenamiento de CO_2 del yacimiento "U Inferior (LU)" e identificar una formación en el tope del reservorio de baja permeabilidad que sea sello para no comprometer la integridad del campo PRH en la Cuenca Oriente.

La información obtenida de pozos perforados, análisis de núcleos, registros, análisis de secciones delgadas y análisis de presiones transitorias, fue empleada para evaluar las propiedades petrofísicas, la calidad del yacimiento y los fluidos del yacimiento. Además, las propiedades petrofísicas se determinaron por diferentes métodos para disminuir la incertidumbre en las mediciones. Todas estas propiedades analizadas se utilizarán posteriormente en el modelo estático y dinámico para comprender el comportamiento del yacimiento "LU" bajo la inyección del CO_2, el cual será utilizado como un mecanismo para aumentar el factor de recobro (es decir, recuperación mejorada de petróleo (EOR) a través de la inyección de CO_2). Se demostró la continuidad y la capacidad adecuada de almacenamiento de CO_2 del yacimiento LU, así como la presencia de una formación de sellado de permeabilidad/porosidad ultrabaja (lutita, caliza) sobre el yacimiento LU lo que proporciona un sistema de almacenamiento geológico seguro para gases de efecto invernadero (GEI). La zona central del campo PRH presenta las mejores características para la inyección de CO_2 debido a las bajas presiones del yacimiento. Adicionalmente, se determinó el azimut que brinda mayor estabilidad al proceso de inyección del gas, evitando la generación de microfracturas en el reservorio y la comunicación de la arenisca con otras formaciones.

El estudio incorporó información existente de la exploración petrolera del campo PRH y se aplicaron diversas metodologías para determinar parámetros petrofísicos. La caracterización de LU proporcionó detalles cruciales sobre el yacimiento, los fluidos y la litología. El volumen teórico de almacenamiento para el yacimiento LU fue de 9,13 millones de toneladas de CO_2. Este trabajo es uno de los primeros en evaluar la captura y almacenamiento de carbono (CCS) en la Cuenca Oriente para reducir el impacto ambiental de las emisiones de GEI.

Palabras clave: CCS; Almacenamiento de CO_2; Almacenamiento geológico; Reservorio; Arenisca; Petrofísica.

1. Introduction.

In Ecuador, GHG emissions for the year 2021 were 37.9 kton of CO_2 eq (Ministerio de Energía y Minas, 2022). This value presents an environmental challenge for the national oil and gas industry.

Geological carbon storage has been considered as a potential technology for slowing down CO_2 emissions to mitigate climate change (Bachu, 2000). Production or depleted hydrocarbon reservoirs are the main option for CO_2 storage due to their geological integrity, physical properties, and adequate structure. EOR methodologies, such as gas injection to improve the sweep efficiency, have been used for many decades (Silva, 2011). The Lower "U" reservoir can be considered as a future CO_2 storage formation which would reduce GHG emissions by utilizing currently gas flaring as the injectant for EOR.

The analysis included 35 wells which produce 4464 BOPD in total (average 10 % BS&W). PRH field has a reservoir depletion (from 3000 to 1300 psi) and oil production decline, trend which makes it a good study candidate.

Geological data will enable the assessment of whether the Lower "U" reservoir meets the criteria for serving as a CO_2 storage site. The reservoir evaluation should consider depth criteria, permeability (K), porosity (Ø), salinity of formation water, and geological structure (Galarza, 2013). Assessing these features in the Lower "U" reservoir is essential to ascertain its stability and safety as a storage facility, providing valuable insights for potential utilization in carbon capture and storage initiatives.

2. Geological Background.

The PRH field was discovered by Texaco-Gulf through the drilling of PRH-1 (depth 10,173 ft) in 1968 (Bady et al., 2014). Seismic interpretation defined the structure as an anticline (oriented N-S, 20 km long with an average width of 4.5 km) with an eastward-dipping reverse fault, having a NNS-SSO direction, as shown in Figure 1.

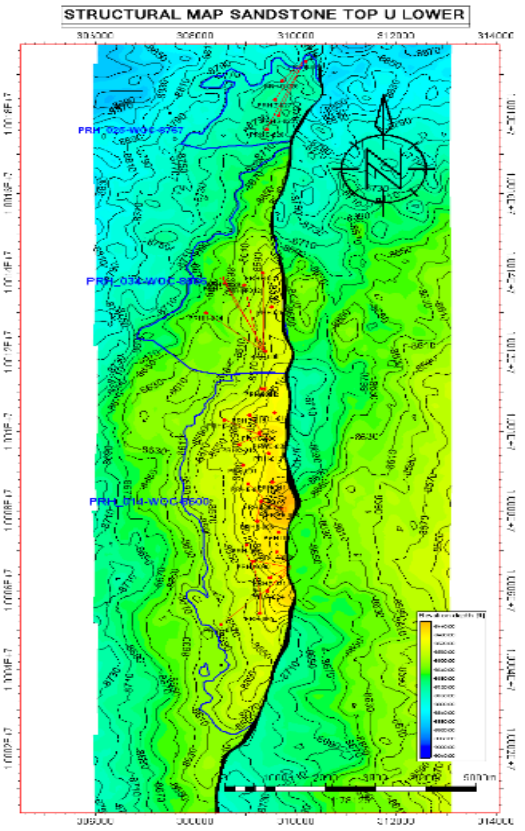

Figure 1. Structural map of the LU sandstone reservoir.

In the PRH field, three compartments were defined: the northern zone, PAD H-central zone, and the southern zone. The analysis focuses on the different behaviors of the producing reservoirs along the structure, influenced by structural changes and validated by variations in fluid salinity, as shown in Figure 1.

The division between the northern zone and PAD H is marked by a structural change observed in seismic data of approximately 90 ft, and they are separated to avoid overestimating the Original Oil in Place (OOIP), constrained by well PRH-25. The PAD H compartment is limited to the south by wells with low prospectivity (e.g., PRH-34) in its main reservoirs and a structural lineament, controlled by the Water Oil Contact (WOC) defined in well PRH-34.

The central-southern zone is controlled by the WOC of the structurally lowest well in the area, well PRH-14 (Loor & Ruiz, 2022), as depicted in Figure 1.

Three hydraulic zones are defined, separated by changes in lithofacies, giving rise to different water-oil contacts in the reservoirs of the Napo Formation (U and T).

The sedimentation environment of the "U" sandstone belongs to fluvial channels and delta bars, with these bars being linked to channels and regressions. The sedimentation direction is almost parallel to the trend of the structure; for this reason, the reservoir varies from one well to another and is divided into:

• **Upper U Formation:** Friable quartz sandstone, light gray, very fine to fine grain, subangular to subrounded, with calcareous cement, showing good presence of hydrocarbons and exhibiting a whitish-yellowish fluorescence.

• **Lower U Formation:** Firm, light brown, monocrystalline quartz sandstone; hyaline, firm, medium-coarse grain, subangular, poor sorting, slightly siliceous cement, with traces of glauconite, saturated with hydrocarbons. It exhibits a quick cut and whitish-yellow fluorescence (Loor & Ruiz, 2022).

3. Geological Structures at the CO_2 Injection Site.

For Characterization and CO_2 Storage (CCS), the reservoir's continuity and connectivity between injection and production wells are crucial. The analysis area is situated on the western flank of the anticline in the PRH field.

A correlation section was defined to visualize the continuity of bodies, with a focus on identifying the consistency in the thickness of the limestones located at the boundaries of each cycle. While the main reservoirs appear somewhat compartmentalized, they exhibit good connectivity, defining minimal accommodation lows. This connectivity is essential for effective CCS operations in the PRH field.

In the PRH field, a pronounced thinning trend is observed in the sands from south to north. The lateral continuity of the Lower U is also reduced compared to the T sandstone, with well PRH-3 exhibiting the thickest sand interval (60 ft).

Applying the concept of sequence stratigraphy, lithotypes were modeled, and a stratigraphic correlation was generated. Figure 2 displays the correlation map of wells PRH-33, 21, 20, 10, 18, 17, 16, 8, 15, 3, and 9, covering the entire field from north to south. This correlation map provides insights into the distribution and variations in lithotypes across the PRH field, aiding in understanding the stratigraphic complexities and thinning trends.

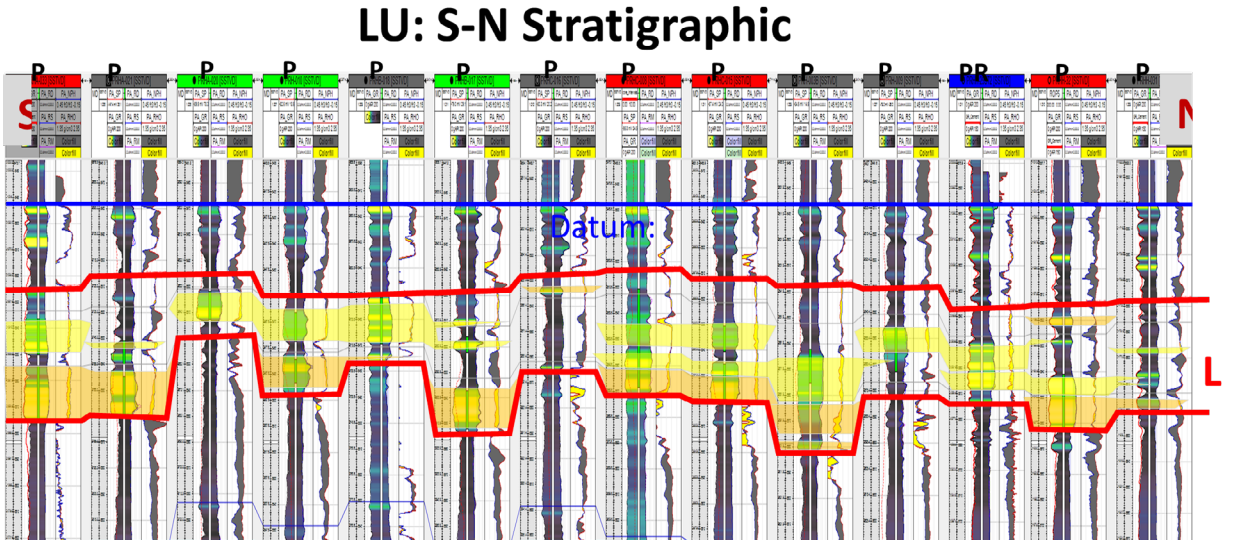

Figure 2. U: S-N Stratigraphic cross section.

4. Analysis and Discussion.

4.1. Porosity and Permeability.

The diagenesis of Lower "U" reveals the influence of cementation and compaction on petrophysical properties. This study presents the results of porosity (Ø) and permeability (K) using different methodologies. These parameters are necessary for calculating CO_2 storage capacity. This analysis is crucial because petrophysical properties are essential characteristics in the configuration of reservoir rocks, enabling the prediction of fluid behavior within the reservoir (Catziz & Tobon, 2016).

Changes in sedimentation or deposition conditions can lead to variations in porosity across different sectors of the reservoir. Sediment heterogeneity is a crucial consideration in these analyses (Castillo & Ortega, 2016). The reservoir's quality and the continuity of the LU sandstone determine the volume of CO_2 that can be stored.

The acquisition methods of data provide information at different scales. Core measurements offer insights into a very small sample, while well geophysical logs provide information on a larger rock volume.

Porosity and permeability were determined using core analysis from wells and open hole well log analysis. The integration of information from both direct and indirect methods was employed to establish representative values for LU (Figure 3).

The study also incorporates a well test analysis (Build Up) that provides valuable information, particularly due to its scale, allowing focused insights into the productive sandstone (Castillo & Ortega, 2016).

The initial analysis focuses on diagenesis to understand its influence on petrophysical parameters defining reservoir quality.

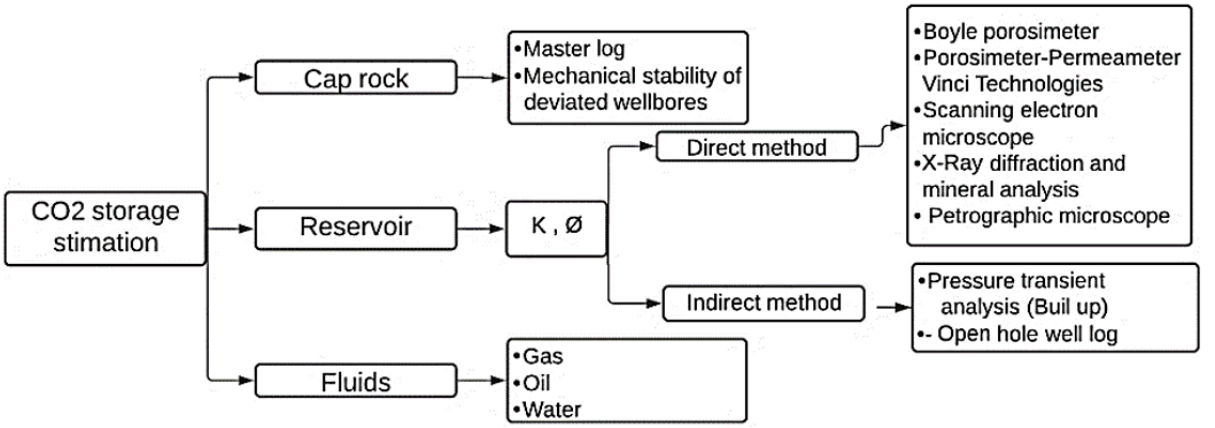

Figure 3. Methods for estimating petrophysical parameters.

4.2. Diagenesis.

The diagenesis of the rocks has a direct influence on the properties of the rocks and therefore on the quality of the reservoir. Cementation, for example, can significantly alter the quality of a reservoir and intense compaction can reduce porosity (Wang et al., 2019).

In the petrographic analysis of Lower "U" at well PRH-8, two main lithologies were identified: quartz sands and calcareous quartz sands. The mineralogical composition is predominantly characterized by monocrystalline quartz, with some sectors displaying fracturing and secondary growth of quartz grains. Grain sizes range from lower fine to upper fine and lower coarse.

The observed contacts exhibit various characteristics, including point contacts that are concave or convex, both in specific sectors and throughout the formation. Additionally, floating contacts were noted in the calcareous quartz sands (Endara, 2015).

The diagenetic processes analyzed in the sedimentological study based on core samples involve physical, chemical, and biological aspects. The dominant physical process is mechanical compaction. Among the chemical processes, primary siliceous cementation is noted, along with significant secondary calcareous cementation and minimal pyrite authigenesis. In terms of biological processes, marginal sandy sediments show minimal bioturbation. Sorting is moderate to good. The matrix is composed of clays deposited in intergranular spaces or resulting from feldspar dissolution.

Siliceous cement is typically quartz deposited as overgrowth on the grains. A summary of the characteristics is presented in Table 1.

Table 1. Textural characteristics PRH-8 (Endara, 2015).

Depth	9552	9554	9555	9555.5	9556	9560	9561.3
Rock type	Quartz arenite	Quartz arenite	Quartz arenite	Quartz arenite	Quartz arenite	Quartz arenite calcareous	Limestone
Grain size	Fine	Fine	Fine	Fine	Very fine	Medium	Very fine
Roundness	SBA - SBR -R	SBA - SBR -R	SBA - SBR -R	SBA - SBR -R	SBA - SBR -R	SBA - SBR	SBR
Sorting	Well	Well	Well	Well	Well	Well	Moderately
Matrix rock	Clay	Clay	Clay	Clay	Clay	-	-
Cements	Silicious calcareous	Silicious calcareous	Silicious calcareous	Silicious calcareous	Silicious	Silicious calcareous	Silicious clayey
Porosity (%)	15	15	10	10	8	1	Traces
Maturity	Mature	Mature	Mature	Mature	Mature	Mature	Mature

Primary compaction, along with quartz overgrowth followed by calcite precipitation, are the main causes of the loss of primary intergranular porosity (Estupiñan et al., 2006), with Ø ranging from 15 to 10 %.

4.3. Sedimentological Analysis

In the Core analysis of PRH-8 (13 ft), 43 % consists of sandstones, 37 % are fine clayey sediments, and certain intervals are interspersed with laminations of fine sandstone, while 20 % comprises calcareous sediments (shell remnants and small bivalves, inoceramus). In terms of texture, the grain sizes of the sandstones have a classification ranging from moderate to good, and sporadically poor. The grains are subangular to subrounded, locally angular, rounded, with a moderate to hard consolidation (Table 2).

The grain size is mainly between fine lower to upper, with a smaller proportion of medium lower to upper, sporadically coarse lower, and scattered coarse upper grains. The roundness of the grains in these sandstones varies from subangular to subrounded, locally angular, and rounded. The sandy sediments exhibit a preferentially moderate to hard consolidation (Table 2).

Table 2. Microscope rock texture characterization PRH-8 field (Montenegro et al., 2015).

Depth (ft)	9552	9553	9554	9555	9555.1	9555.5	9556
Rock type	QA	QA	QA	QA	QA	QA	QA
Gain size	Fine / Very fine	Fine / Very fine / Medium	Fine / Very fine / Medium	Fine / Very fine / Medium	Fine / Very fine	Very fine / Medium	Fine / Very fine
Roundness	SBA-SBR	SBA-SBR	SBA-SBR	SBA-SBR	SBA-SBR	SBR	SBA-SBR
Sorting	Well	Moderately	Moderately	Moderately	Moderately	Moderately	Moderately

4.4. Lithological Composition, Texture, and Color of Sandstones.

The analysis is conducted on the sandy intervals of the core (each foot or half-foot), with emphasis on granulometric changes. The sandstones exhibit a modal lithological composition consisting of:

Quartz (58-97 %, variable), glauconite (Traces (Tr)-1 %), clay matrix (Tr-3 %, typically 2 %), micas (Tr-1 %, muscovite and sporadically biotite), framboidal pyrite (Tr-1 %), organic matter (Tr-1-2 %, in the form of coal laminations), residual hydrocarbon (Tr-locally 30 %, typically 2 %, tar), potassium feldspars (locally kaolinized) and plagioclase (Tr-1 %), calcareous cement (20-40 %, middle part of the core) (Montenegro et al., 2015).

Due to hydrocarbon impregnation, the color of the sandstones ranges from light to very light brown (Figure 4.1), sporadically gray to light gray, exhibiting good saturation (residual hydrocarbon, Figure 4.2), and white (considerable residual cement, Figure 4.3) (Montenegro et al., 2015).

Lower "U" includes some minerals (feldspars, plagioclase, mica) referenced in the research findings "Evaluation of the CO_2 Storage Capacity in Sandstone Formations". Research indicates that minerals such as calcite, dolomite, and clay formed as a result of a reaction between CO_2 and other minerals (K-feldspars, plagioclase, epidote, serpentine, chlorite, and mica) are environmentally friendly minerals (Christopoulou et al., 2011).

Figure 4. Core photographs of fine-grained sandstone showing hydrocarbon accumulation in LU.

Between the petrographic-diagenesis and sedimentological analyses, there is a noticeable similarity in describing the textural characteristics of Lower "U" and the influence that physical, chemical, and biological diagenetic processes have on the reservoir.

For Lower "U", a high content of sandstones is defined, with a notable presence of fine clayey sediments and, to a lesser extent, calcareous sediments. In terms of texture, grain sizes indicate low variability, generally moderate classification, and roundness ranging from subangular to subrounded.

Additionally, information from various studies conducted on Lower "U" is included, focusing on characterizing petrophysical parameters and determining their influence on the reservoir:

In the thin section analysis, it was observed that the porosity is of intergranular type, with elongated shapes, heterogeneously distributed, and poorly interconnected. Locally, it is reduced or obstructed by organic matter, silts, or secondary overgrowth of quartz grains. Porosity varies from traces to 15 % (good Ø). Secondary porosity is observed in clays (Endara, 2015).

Geological core analysis was applied to wells PRH-8 and PRH-2 to determine the effective porosity and absolute permeability of Lower "U". Seven samples from the interval at 9552 and 9564 ft were considered, and experimental measurements of porosity, grain density, and absolute permeability were determined using the Boyle porosimeter. A linear regression determined the equation correlating effective porosity with absolute gas permeability (Eq. 1). Additionally, absolute permeability and Klinkemberg permeability (Porosimeter-Permeameter) were found. Eq.1 Correlation

$$\emptyset_e - K_{abs}$$

$$k = 1.0465 * e^{(0.3659*\emptyset)}$$

$$R^2 = 0.9984 \quad (1)$$

Table 3a shows the results of absolute permeability and Klinkemberg permeability; in well PRH-2, the two measurements are similar, indicating a high permeability of 384 and 371 mD. A value of 285 mD was obtained in PRH-8, with the estimated porosity being 16 % (good porosity) (YACIMIENTOS-CIGQ, 2015).

Table 3. Conventional core analysis and average petrophysical parameters interpretation (YACIMIENTOS-CIGQ, 2015).

(a) LU core analysis

Well PRH-8			Well PRH-2	
Ø (%)	K (md)	Density (g/cc)	K (md)	Klinkemberg PermeabilIty (mD)
16.05	285.53	2.64	384.67	371.91

(b) Average petrophysical interpretation LU

Well	Ho (ft)	Φ (%)	Sw (%)	K (mD)
PRH-9	8.33	11.6	16.62	43.77
PRH-8	12	12.7	18.9	124.2
PRH-2	24	11.3	37.67	71.24
PRH-14	13.77	15.3	34.3	637.13
PRH-25	12	13.86	37.19	111.11
PRH-34	2.42	11.17	43.45	118.77

The petrophysical analysis of PRH-9 (Figure 5), indicates a formation with relatively clayey developments, featuring variable thicknesses ranging from 4 ft to approximately 30 ft, predominantly composed of clays, mudstones, and fine to medium-grained clayey sandstones, with sporadic intercalations of medium to coarse-grained quartz sandstones and calcareous sandstones. The latter correspond to the oil-bearing thicknesses in wells PRH-3 and PRH-8.

The average porosity is 11.6 % (regular Ø), water saturation is 16.6 % (Table 3b), and the oil-water contact (OWC) is located at approximately 8767 ft True Vertical Depth (TVD). Table 3b includes petrophysical parameters from 6 wells in PRH, all of which exhibit excellent permeability.

The permeability map of Lower "U" was generated from the petrophysical interpretation of well logs. To the east of the fault, permeability exhibits better characteristics, decreasing from south (300-600 mD) to north (25-200 mD), and the central zone has a permeability ranging between 25-200 mD, as shown in Figure 5.

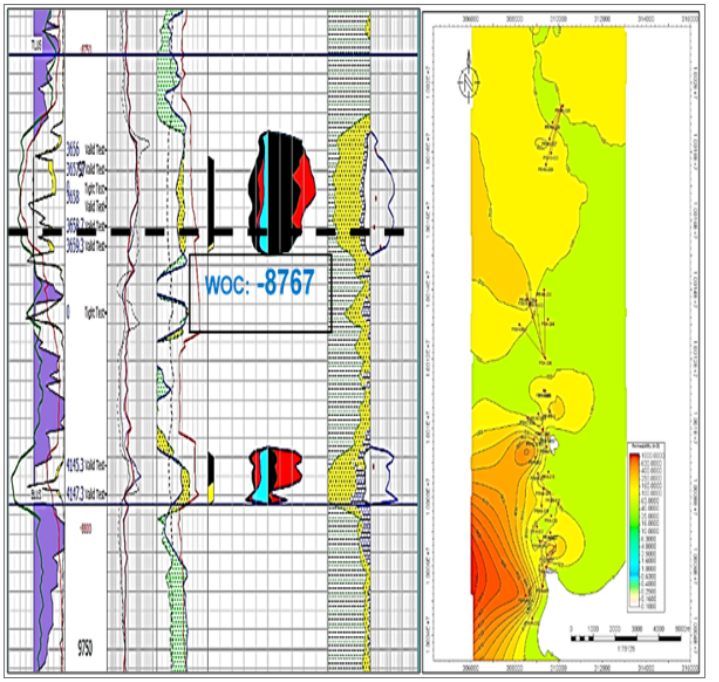

Figure 5. Petrophysical analysis of well log and permeability map LU.

Scanning Electron Microscope (SEM) analysis was conducted on 8 samples (9552 - 9564 ft). The samples correspond to grain-increasing strata at the top of very fine to fine sandstones, which are subangular, with regular sorting, elongated and tangential contacts, siliceous cement, somewhat calcareous (Figure 6a). At depths of 9561.3 and 9564 ft, the strata consist of shale. Quartz is the predominant mineral and exhibits secondary overgrowths, influencing the porosity of the sandstone (Figure 6b) (Toala & Coello, 2008).

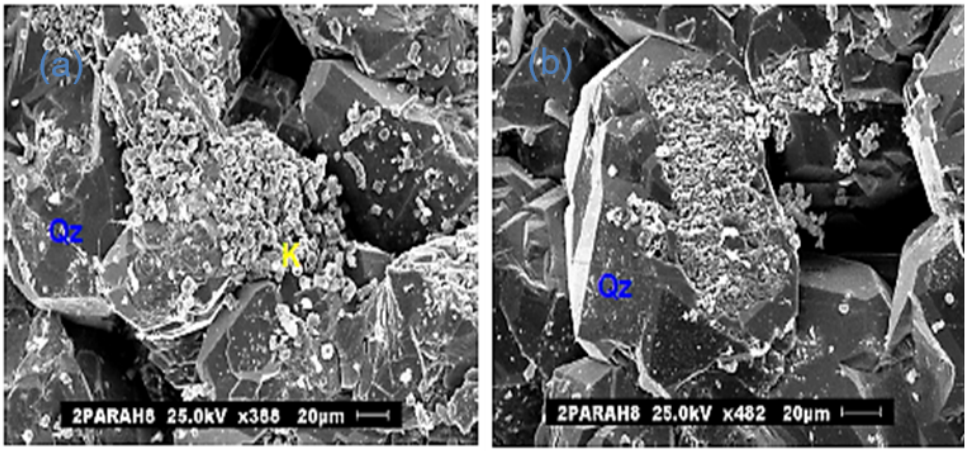

Figure 6. (a) Very fine-grained sandstone with regular sorting and subangular grains. Kaolinite (K) is observed. (b) Secondary overgrowth and erosion of the quartz (Qz) surface (Toala & Coello, 2008).

The porosity varies from 3 to 5 % (very poor porosity), being null at depth; the average pore diameter is 40 µm, and clay content is 8 %. The identified clay is kaolinite, primarily originating from feldspar alteration. Kaolinite is present in its plate-like structure, forming discontinuous blocks arranged massively within the intergranular space. Although kaolinite is a chemically stable clay, its high percentage can impact the reservoir's low permeability (Figure 7), (Toala & Coello, 2008).

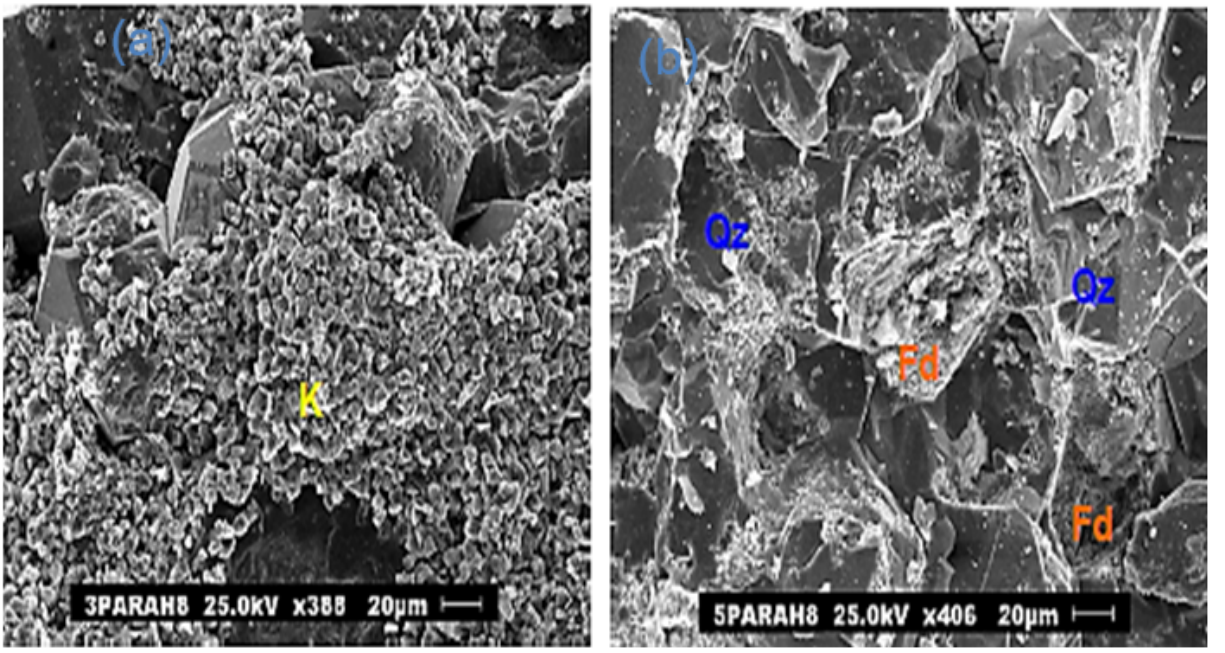

Figure 7. (a) Kaolinite clay (K) found between intergranular spaces. (b) Sandstone with zero porosity. Feldspars (Fd) are observed between quartz grains (Qz) (Toala & Coello, 2008).

X-Ray Diffraction and Mineral Analysis (XRD) reveal a high quartz content (84 %), kaolinite (11 %), and low feldspar content (5 %), as shown in Table 4.

The petrographic microscope was employed to analyze 41 thin-section samples and determine pore size. The lengths of the pores are mostly between 53.4 and 236 µm, and they have been lightly affected by diagenetic phenomena. The pore size measurements are classified as micro and macro pores, granulometrically equivalent to silt to lower-medium sand sizes (Medina et al, 2011). The effects of grain size, packing, compaction, and solution/dissolution processes related to development, preservation or loss of primary and secondary Ø. Additionally, all these processes configure various variations between Ø and K (Ma & Morrow, 1996).

Table 4. XRD analysis mineralogical composition total dust (%) PRH-8 (Estupiñan & Pacheco, 2019).

Depth	Silicate	Phyllosilicate	Carbanate	Tectosilicates		Sulfide
(ft)	Quartz	Kaolinite %	Calcite %	Fpto-K %	Muscovite%	Pyrite/chalcopyrite%
9552.8	84	11	-	5	-	-

4.5. Reservoir Rock

Reservoir quality is primarily controlled by microscopic pore morphology and structural features (Raeini et al., 2015). The reservoir quality of Lower "U" is influenced by grain size and matrix content, parameters controlled by sedimentary and diagenetic processes, primarily compaction and cementation. The quality of interconnected (effective) reservoir porosity is reflected by the estimated and petrographically observed porosity values (Endara, 2015).

The color of the sandstones results from hydrocarbon impregnation and displays shades ranging from light to very light brown, sporadically gray to light gray, indicating good saturation. The few millimeter-scale silty and carbonaceous laminations, as well as minimal bioturbation present, would not significantly affect the petrophysical conditions of the reservoir (9552 - 9555.5 ft). Considerable calcareous cementation is observed in sandstones towards the base of the core (Figure 4). The sedimentary paleoenvironments identified in this core are marine and transitional or marginal (Montenegro et al., 2015).

SEM analysis of the core concludes that Lower "U" does not exhibit excellent reservoir characteristics. The primary diagenetic process affecting the reservoir is the secondary overgrowth of quartz, minimizing permeability, and the presence of clay within the pores results in minimal porosity.

When clay minerals are predominantly present along the walls of the pores and throats, clay plays a crucial role in influencing fluid seepage (Zheng & Liu, 2015). Additionally, poor physical properties, small throats, complex pore structures, and strong heterogeneity in tight sandstone can pose a series of complex challenges for oil and gas exploration and development (Olson, 2009).

The clay content in Lower "U" reduces storage capacity; however, the parameters identified in PRH are acceptable. Lower "U" produces 223 bopd from 5 wells, indicating that the reservoir has permeability sufficient for fluid displacement. Furthermore, the sandstone has good hydrocarbon saturation despite not having high porosity. These petrophysical characteristics are favorable for CO_2 injection and oil recovery.

The Build Up analysis (PRH-32) involves studying the derivative curve, the diffusivity equation, and the data to determine that the pressure restoration curve takes on the typical shape of a fault (Figure 8), exhibiting radial flow before the shut-in time.

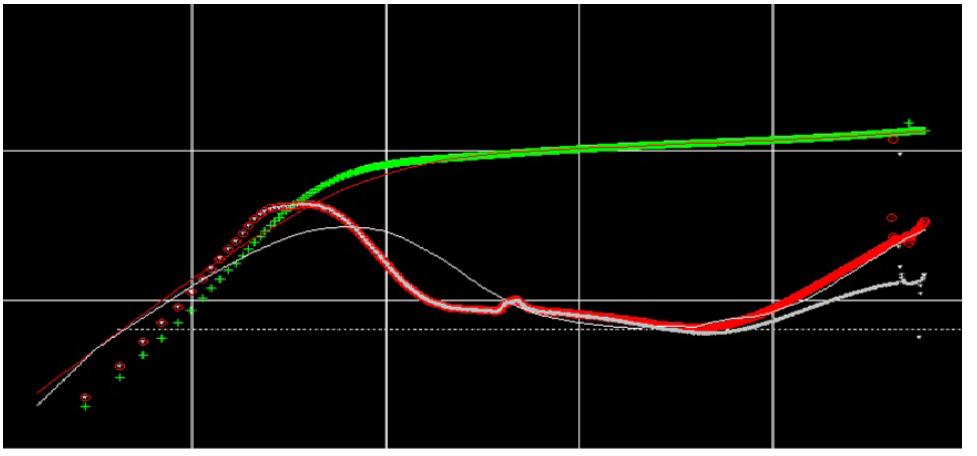

Figure 8. LU Build Up - pressure curve and derivative curve PRH -32.

The model used is a homogeneous reservoir intersected by faults and considers oil production. A permeability (K) of 43 mD, effective porosity of 10 % (regular porosity), and a formation damage of 4.45 (S>0, permeability reduction) were obtained, as shown in Table 5. Similar results of permeability and porosity were observed in four other analyzed wells.

Table 5. Pressure buil Up test analysis, PRH-32- LU.

Pwf (psi)	Reservoir Pressure (psi)	J (stb/psi)	kh (mD. Ft)	k (mD)	Skin	Effective Ø (%)
1380	3131	0.32	643	42.8	4.45	10.3

4.6. Reservoir Pressure

In the Napo formation (U, LU, Upper T, and Lower T), the production behavior and reservoir pressures (Figure 9) confirm that the production mechanisms involve rock-fluid expansion, gas in solution, and a partial water drive contribution.

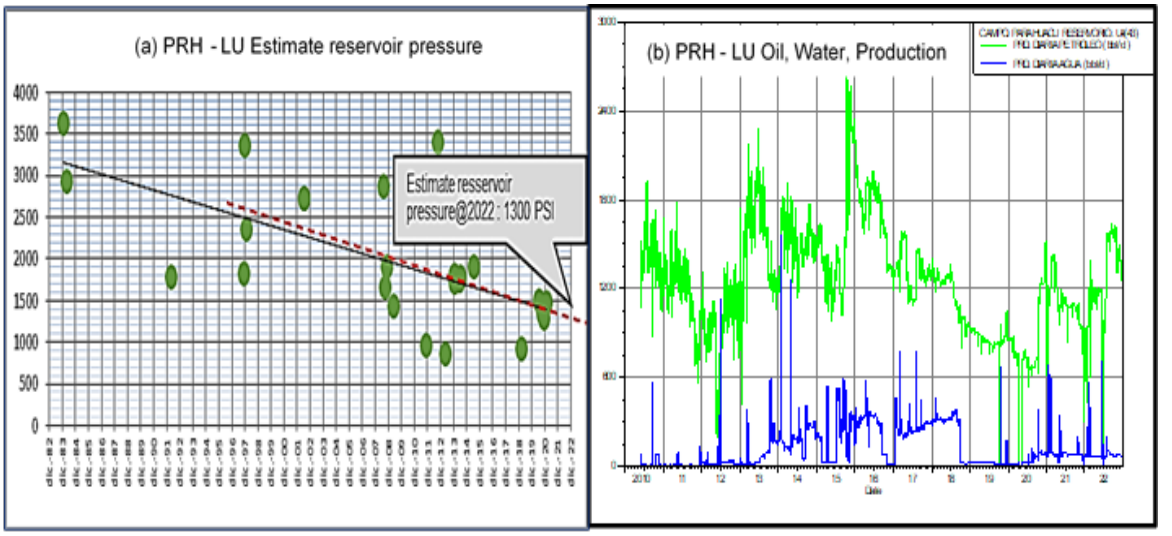

Figure 9. LU Reservoir pressure - oil and water production.

The energy of Lower "U" is depleting, influencing a decrease in production (Figure 9). The average pressure approaches the bubble point pressure (1485 psi), forming a gas cap around the wells and causing a production decline (Loor & Ruiz, 2022). The estimated initial reservoir pressure for December 2022 was determined to be 1300 psi (Figure 9a).

The Build Up analysis of PRH-13 (860 psi) and PRH-18 (1740 psi) located in the southern part confirms that pressures are approaching the bubble point. On the other hand, PRH-32 has a high reservoir pressure of 3131 psi as it is a new well drilled in 2022; however, its reservoir pressure will decline rapidly, leading to a decrease in production, which is typical for the PRH field. The analysis considered pressure data since 1983, and at that time, the initial reservoir pressure was 3782 psi at a reference datum of 8570 ft.

In fig. 10, it is observed that in the northern and central zones, pressures exceed 2000 psi due to recent oil exploration. The southern zone has depleted pressure values due to reservoir energy depletion from being in production for more years.

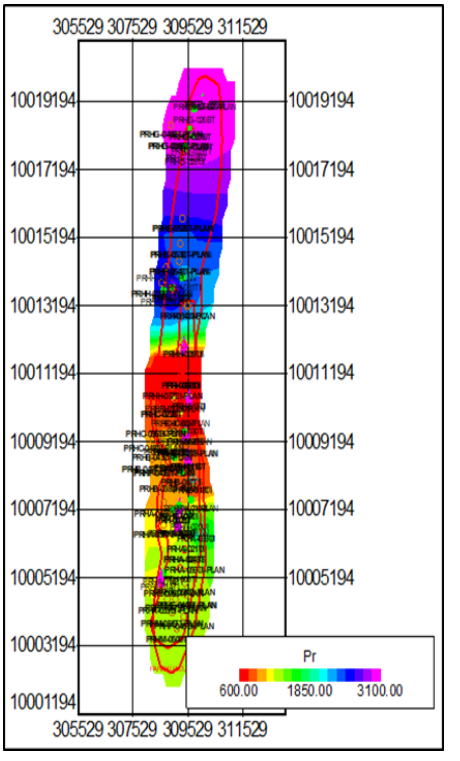

Figure 10. Reservoir pressure distribution in LU.

Due to the decline in production in recent years (2015-2020, Figure 9b), there is consideration for implementing an Enhanced Oil Recovery (EOR) pilot project to increase the recovery factor by injecting CO_2.

The principle of miscible gas injection lies in reducing interfacial tension between fluids and eliminating capillary forces. Injecting CO_2 into the formation has become one of the preferred methods worldwide (Ayala & Andrade, 2017). The CO_2 for injection will be obtained from flare gas from neighboring wells to reduce greenhouse gas emissions to the environment.

In CO_2 injection, pressure and depth directly affect the CO_2/water formation saturation, which is a challenging parameter to characterize, introducing uncertainty in estimating CO_2 storage capacity (Hurtado, 2009). Additionally, pressure changes and geomechanical effects caused by hydrocarbon production in the reservoir can reduce the volume of CO_2 that could be stored (Chadwick, 2007). For this reason, this study presents the current pressure situation in Lower "U", and based on the aforementioned, it can be affirmed that PRH field is a good candidate for CO_2 storage. It favors conditions for maintaining CO_2 in a supercritical state, as indicated by the methodology for storage in permeable formations by Hurtado. Lower "U" meets the pressure (1058.7 psi) and temperature (87.3 °F) values above its critical points, with the sandstone averaging 208 °F and 1320 psi.

4.7. Seal Rock Integrity for CO_2 Geological Storage

Designing secure storage is the first step to ensuring success in a CCS project. The caprock, faults and fractures are parameters that define safe storage. A rock with poor petrophysical characteristics is an excellent seal rock, and the quality of the seal is given by the geometry and integrity of the seal (Endara, 2015).

Some characteristic of the geology of the reservoir provide security for the confinement of CO_2 but present operational challenges, for example, seal rocks rich in clay may have a reduced pore size, this combination of parameters causes high capillary pressures, additionally drag as a consequence of viscosity increases and the mobility of fluids in the reservoir is limited (Espinoza & Santamaria, 2017).

At the top of hydrocarbon reservoirs it is common to find mud rocks and evaporites, one of the main components of mud rocks is clay (Guéguen & Palciauskas, 1994). One of the parameters that define the quality of a reservoir is the size of the pores and this is influenced by cementation, diagenesis, depth and compaction wich can reduce the porosity (Nygaard et al., 2004). Additionally Ø decreases exponentially with effective stress (Chong & Santamaria, 2016).

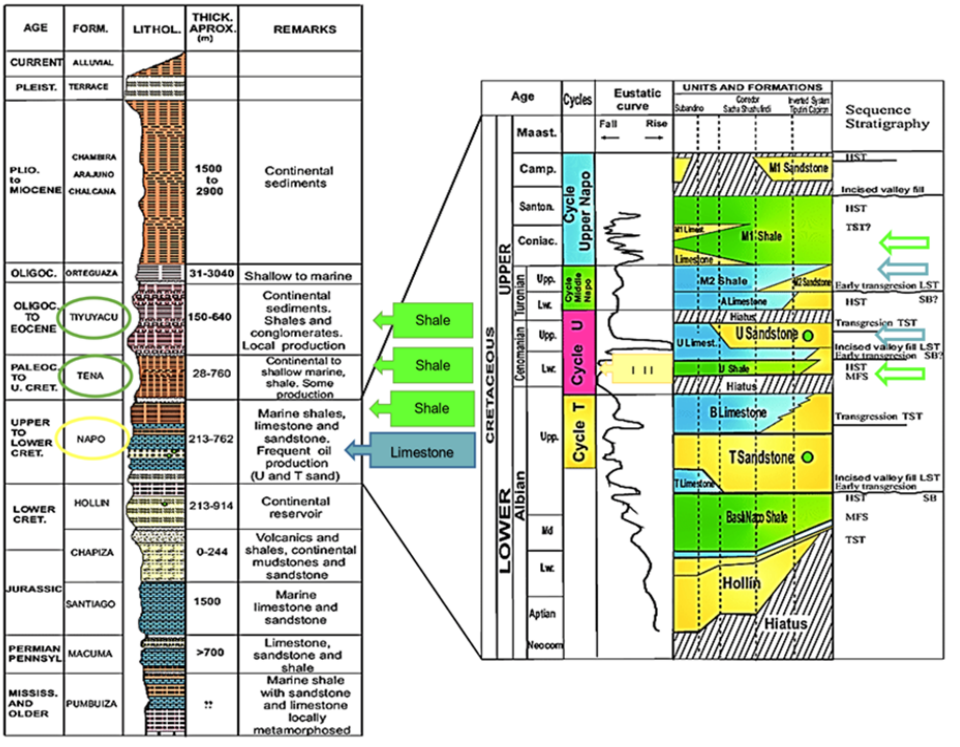

Figure 11. Generalized stratigraphic column, Oriente Basin-Ecuador (Estupiñan et al., 2010).

Lower "U" (fig. 11, yellow sandstone) is at an average depth of 11,500 ft Measured Depth (MD), isolated from the surface and freshwater-bearing formations by significant impermeable formations within the Tertiary formations deposited over the Tiyuyacu formation. These include the clays of the Tena formation, shales (Figure 11, green), and upper limestones (Figure 11, blue) of the Napo formation. All these features, along with a limited extent of the existing main fault that does not reach the surface, create different zones of low permeability, preventing the injected CO_2 from ascending to shallow aquifers and the surface.

In the master log of the last drilled well (PRH-32), it is observed that LU is confined at the top by limestone A, limestone M2, and limestone M1, and at the base by limestone B. These lithologies are impermeable strata, and indeed, these impermeable lithologies provided the seal in the petroleum system of the LU reservoir (Figure 12), Additionally, it is important to emphasize that in the three fields (LGA – GNT - PRH) comprising Block 56, there are no outcrops of LU. Therefore, lateral contact with freshwater reservoirs is improbable.

The structures responsible for oil accumulation in PRH field, and generally throughout the Sacha-Shushufindi structure, exclusively affect pre-Cretaceous formations and the basal terms of the Cretaceous, without any influence on the sedimentary sequence from the Tertiary to the present.

The potential freshwater reservoirs (shallow aquifers) are entirely disconnected from the productive oil zones. Over 8000 ft of rock column separates the hydrocarbon-producing sandstone from the shallow reservoirs (E.P. PETROECUADOR, 2022), and more than 11,500 ft (MD) from the surface.

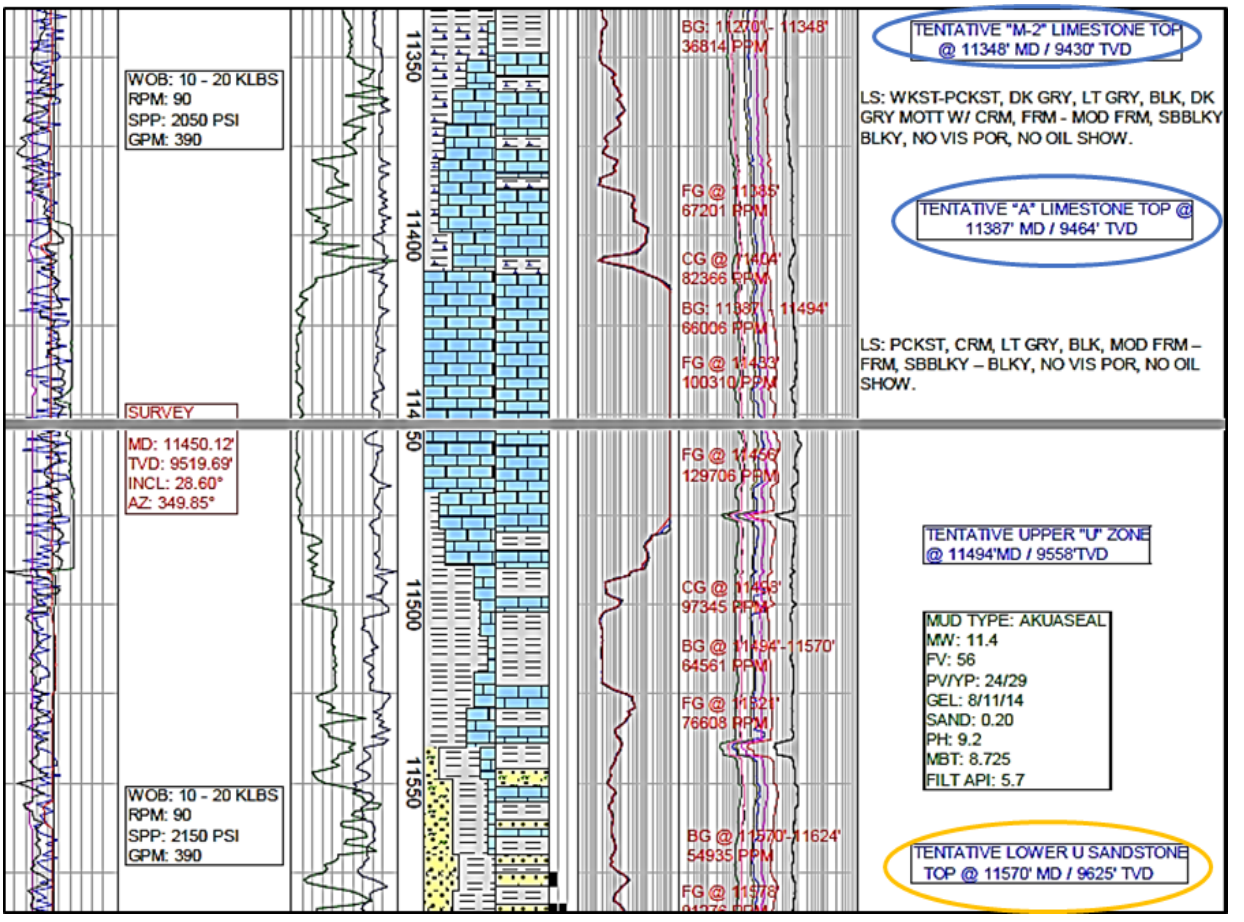

Figure 12. Master log, LU and cap rock section , M-1, M-2, A; PRH-32.

Regional stress regime, faults and fractures affect the geomechanical properties of the cap rock. The magnitude of the pressure on the caprock depends on its K, the location of the injection well. Analyzing the geomechanical properties of the rock under the effects of CO_2 injection is essential to identify changes in the integrity of the cap rock. Changes in stress state with CO_2 injection, and changes in material properties are some of the variables that must be analyzed (Kaldi et al., 2013).

Injection pressure can have secondary effects on the seal rock such as mechanical deformation or damage to the seal. Pre-existing faults or fractures can be activated, this condition can be unsafe and does not provide guarantees for storing CO_2 (Kaldi et al., 2013).

At a depth of 8987 ft, a geomechanical study is available. The anticlinal structure of the field under study has a north-south orientation, while the regional formation stresses have an east-west orientation (Ayala et al., 2018).

The mechanical stability graph of deviated wellbores (Figure 13) depicts unstable zones in red and more stable orientations in blue. In this case, from the PRH field, the maximum horizontal stress (SHmax) is at an azimuth of 45 - 225° N. At a depth of 9000 ft, the flanks of greater stability are found at an approximate azimuth between 0 - 90° and 190 - 270°. These orientations provide greater stability and reduce the likelihood of inducing microfractures when injecting CO_2 that could connect Lower "U" with other formations.

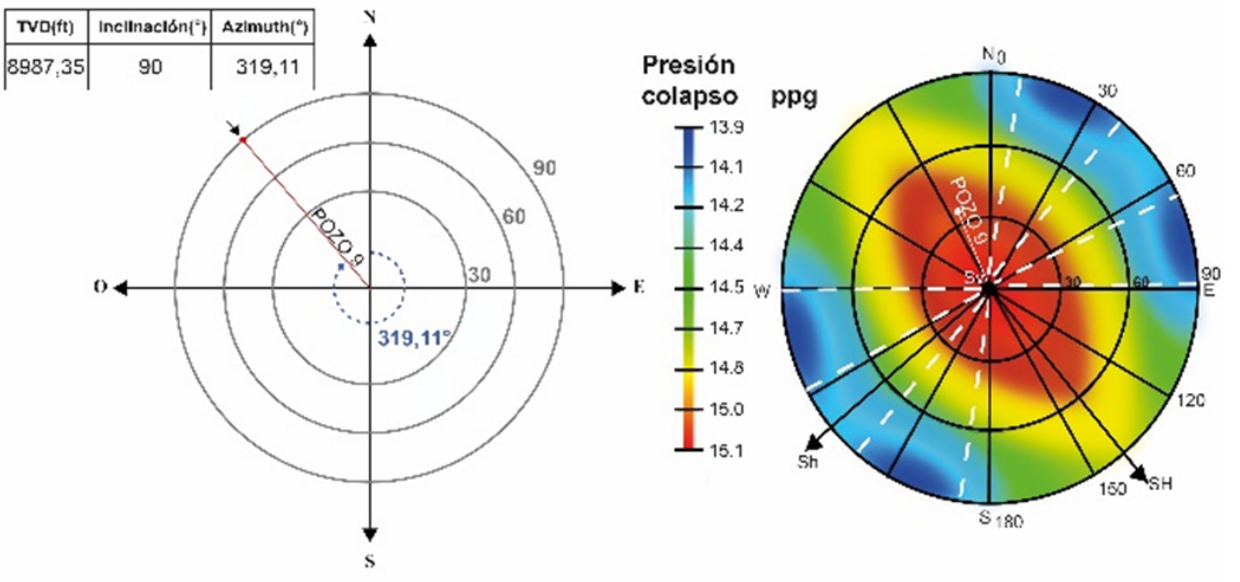

Figure 13. Mechanical stability of deviated wellbores.

4.8. Lower U reservoir fluids

The water salinity varies from 5000 to 87,800 ppm, decreasing from the northern and southern zones towards the central zone. The light oil ranges from 27.8 to 32.6 API and is uniform throughout the field, with an average Gas-Oil Ratio (GOR) of 2000 scf/bbl and a gas production of 1.36 MMscf Figure 14).

Taking into account studies on the influence of connate fluids salinity on the minimum miscibility pressure (MMP) of CO_2, it is noted that CO_2 injection can alter the physico-chemical balance between reservoir rock and formation water, leading to changes in the physical properties of the reservoir rock. Nevertheless, there is a lack of research reporting whether and how these interactions affect the MMP for formations with varying water salinity (Pi et al., 2021). Consequently, the salinity of Lower "U" is not expected to impact the MMP.

The central zone of PRH could store a greater amount of gas, considering that the solubility of CO_2 decreases with increasing water salinity (Galarza, 2013). This concept is not a limitation for considering the entire reservoir.

The PRH field produces the lowest amount of water per day (bwpd) in the entire Oriente Basin, with 532 bwpd, of which 77 bwpd correspond to LU. The Basic Sediment and Water (BSW) does not exceed 2 %. This condition makes the field the best candidate for increasing the recovery factor through secondary recovery and Enhanced Oil Recovery (EOR) due to the limited water potential in the LU sandstone as a result of the partial water drive in the reservoir.

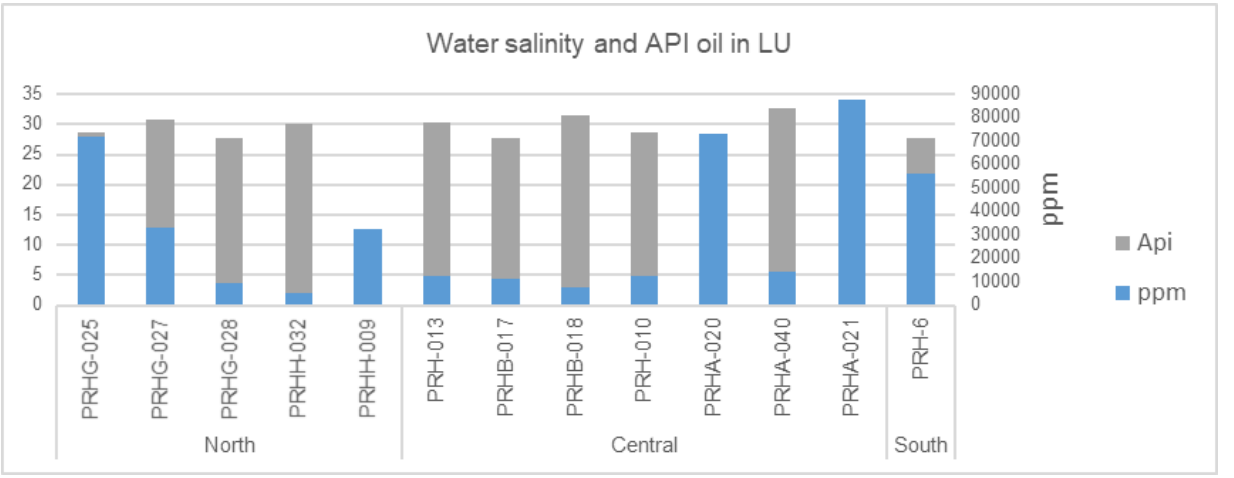

Figure 14. Water salinity and API oil in LU - PRH field.

4.9. CO_2 storage estimation in LU sandstone

According to Ringrose, there are two main trapping mechanisms for CO_2: physical and geochemical. The physical mechanism encompasses (a) regional structural features at a sedimentary basin scale, (b) the geometry of structural and stratigraphic traps, and (c) fluid flow processes, including (i) capillary interfaces between fluids and (ii) the retention of CO_2 as a residual phase. Meanwhile, the geochemical trapping mechanism involves (1) CO_2 dissolution in the brine phase, (2) CO_2 precipitation, and (3) CO_2 adsorption (Ringrose, 2020).

Considering that the Lower U reservoir is a siliciclastic reservoir, insights into the behavior of CO_2 within this type of reservoir were obtained from Baines's research. Baines demonstrates that when CO_2 is introduced into pure quartz sandstones, it remains as a separate phase once the formation water is saturated with CO_2. Some minerals can be diluted by injecting CO2, such as carbonates present in rock cement., but once the formation water becomes CO_2 saturated, the remaining injected CO_2 also persists as a separate phase (Baines & Worden, 2004).

Wikilson's findings indicate that geochemical reactions are slow and relatively minor, typically accounting for less than 5 %. The majority of CO_2 in the free phase ranges between 80 to 95 %, with only around 2.4 % stored in the mineral phase, similar to the dissolved quantity (Wilkinson et al., 2009).

In summary, while geochemical aspects of CO_2 storage can occur, the reaction rates are very slow, and the amount stored is approximately 5 %.

Storage capacity can be estimated using reservoir simulation or analytical approaches. In the subsequent paragraphs, an analytical method has been applied to estimate the amount of CO_2 that could be stored in the Lower U sandstone.

With the aforementioned background, the capacity for the Lower U reservoir in the PRH field has been estimated using the analytical approach for CO_2 in the free phase within a structural trap. Other trapping mechanisms were not considered in this study.

Additionally, adopting the terms proposed by Bachu, as shown in Figure 15, the Effective capacity for the Lower U reservoir in the PRH field has been estimated (using cut-off criteria).

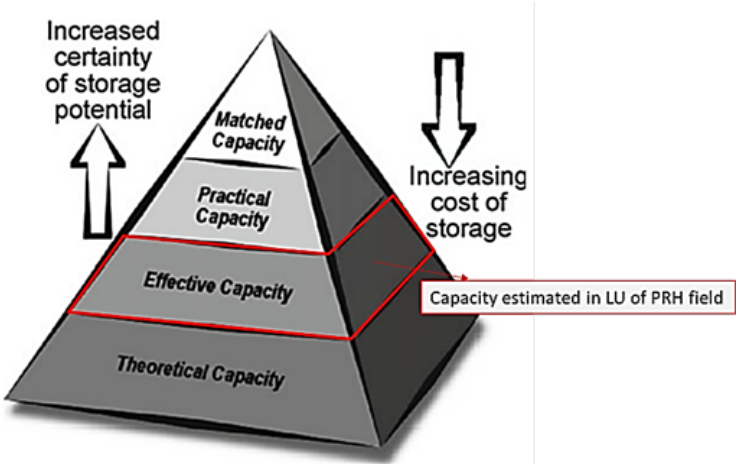

Figura 15. Techno-economics capacities pyramid (Bachu et al., 2007).

4.10. The input values were derived from the LU sandstone

The area corresponds to the structural closure observed at the top of the Lower U depth structure map, initially measured in acres, with thickness in feet. However, these measurements were subsequently converted to square meters (m^2) and meters (m) respectively, yielding the following:

A: 9987 ac = 40,416.39 m^2; thickness: 42.45 ft = 12.92 m, see in right table of Figure 16.

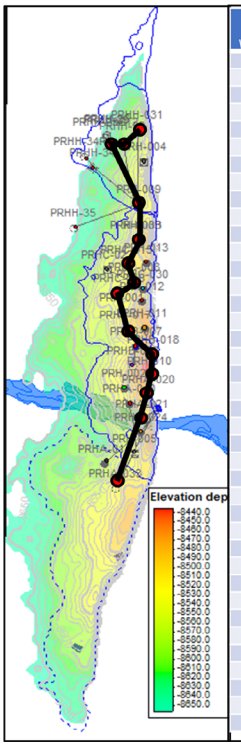

Well identifier	Gross Sand (ft)tvd	Net Sand (ft)tvd	N/G
PRH-001	55.5	22	0.40
PRH-002	53.1	26	0.49
PRH-003	67.5	23	0.34
PRH-003B	65.6	27	0.41
PRH-004	33.3	12	0.36
PRH-005	38.3	16	0.42
PRH-009	41.5	9	0.22
PRH-010	37.3	21	0.56
PRH-011	39.6	19	0.48
PRH-012	56.5	20	0.35
PRH-013	44.7	29	0.65
PRH-025	41.4	20	0.48
PRH-23	48.4	16	0.33
PRHA-014	40.5	17	0.42
PRHA-020	18.2	9	0.49
PRHA-021	54.3	20	0.37
PRHA-024	37.8	21	0.56
PRHA-040	38.9	11	0.28
PRHB-006	29	18	0.62
PRHB-007	13.5	10	0.74
PRHB-017	55.4	30	0.54
PRHB-018	24.7	13	0.53
PRHC-008	48.7	30	0.62
PRHC-015	48.5	30	0.62
PRHC-016	37.3	8	0.21
PRHC-022	30.9	18	0.58
PRHC-030(19)	45.6	16	0.35
PRHG-026	23.7	0.00	0.00
PRHG-027	41	23	0.56
PRHH-31	43	4	0.09
PRHH-29	46.7	31	0.66
PRHH-29ST2	37.8	16.6	0.44
PRHH-32	43.7	19.1	0.44
PRHH-34	44.6	4	0.09
PRHH-34RE	40.1	12	0.30
PRHA-33	50.4	18	0.36
PRHH-35	45.3	34	0.75
PRHH-36	41.2	24.5	0.59
PRHG-028	53.8	21	0.39

Figure 16. Left: 3D view of 4 ways structural closure of LU sandstone. Right: Gross and net sand thickness and N/G ratio.

The CO_2 density at injection depth was read from the following Density-Pressure cross plot, but extrapolated to the TVD injection depth of Lower U reservoir, assuming 10 feet below the structural closure, which correspond to 8690 ft TVD, which transformed to meters is 2649 m TVD, see the dotted square of Figure 17. Additionally, the real conditions of Snohvit CO_2 project were taken as reference, since it has been injected since June 2008 at a depth of 2400m TVD.

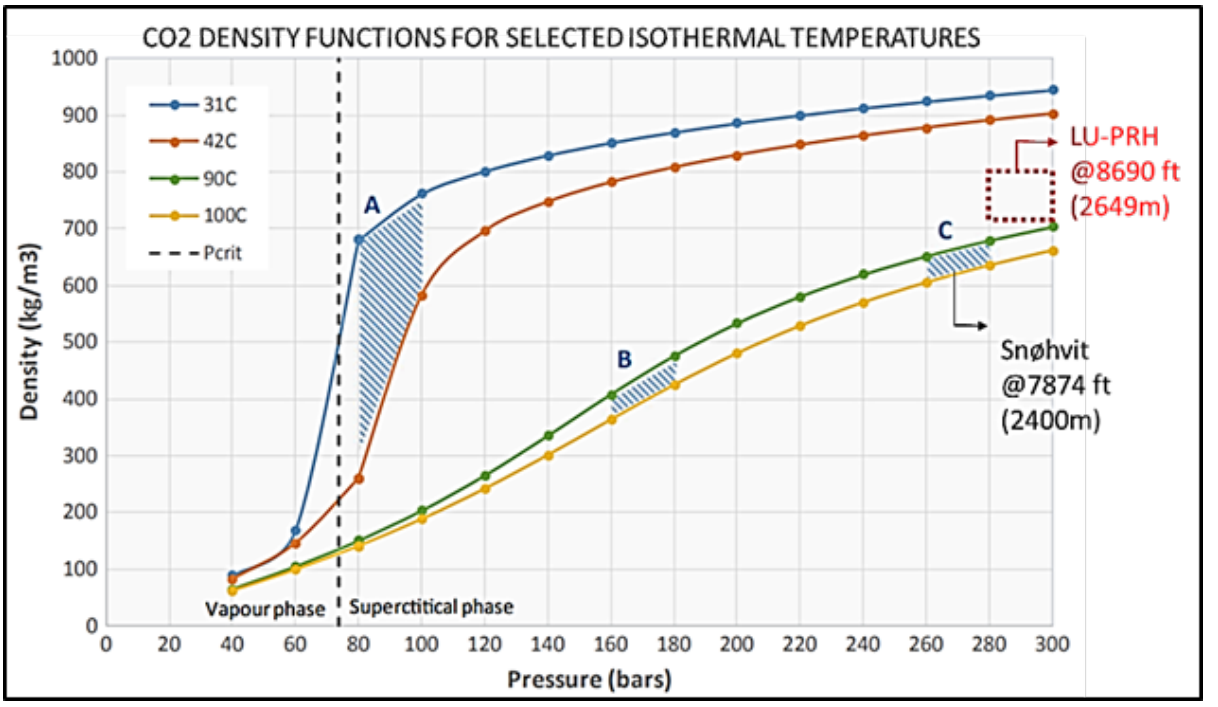

Figure 17. Density-Pressure crossplot showing properties of pioneer CO_2 storage projects; (A) Sleipner, (B) In Salah, (C) Snøhvit. In red square the proposed conditions used in LU estimations (Ringrose, 2020).

The formula used for the current estimation was as follow Eq. 2.

$$M_{CO_2} = V_b \times \varphi \times \frac{N}{G} \times \rho_{CO_2} \times \varepsilon \times (1 - S_{wirr}) \quad (2)$$

All the variables values for LU reservoir of PRH field were as follow:

Table 6. Variables, description and values used for LU storage capacity analytic approach estimation.

Expression Variable	Description	LU- PRH Value
MCO_2	CO_2 Storage Capacity (tonnes)	9,138,220.1
Vb	Bulk rock volume (m^3)	522,179,829.9
Φ	Porosity (dec)	0.119
N/G	Net to gross ratio (taking away the shale content)(dec)	0.43
ρCO_2	Density of CO_2 at injection depth (kg/m^3)	760
ε	Effective storage capacity of the available pore volume	0.60
Swirr	Irreducible water saturation (dec)	0.25
(1 − Swirr)	Maximum CO_2 saturation at the pore-scale (dec)	0.75

4.11. Results of Lower U sandstone CO_2 Analytical Approach

Once every variable of expression was obtained, they were standardised at the same units, then multiplied, the CO_2 storage capacity that Lower U Sandstone Reservoir of PRH field was estimated in 9.13 million tonnes of CO_2 ($MtCO_2$), see Figure 18. This value must be corroborated or contrasted with the 3D static model analysis in future studies.

Objetive	Area (m2)	Gross thickness (m)	Porosity (dec)	Sw=1-So (dec)	NtoG (dec)	CO2 Density (kg/m3)	Effective (dec)	MCO2 (Kg)	**MCO2 (tonnes)**
MCO2 - LU	40416396	12.92	0.119	0.25	0.43	760	0.6	9138220129	**9 138220**

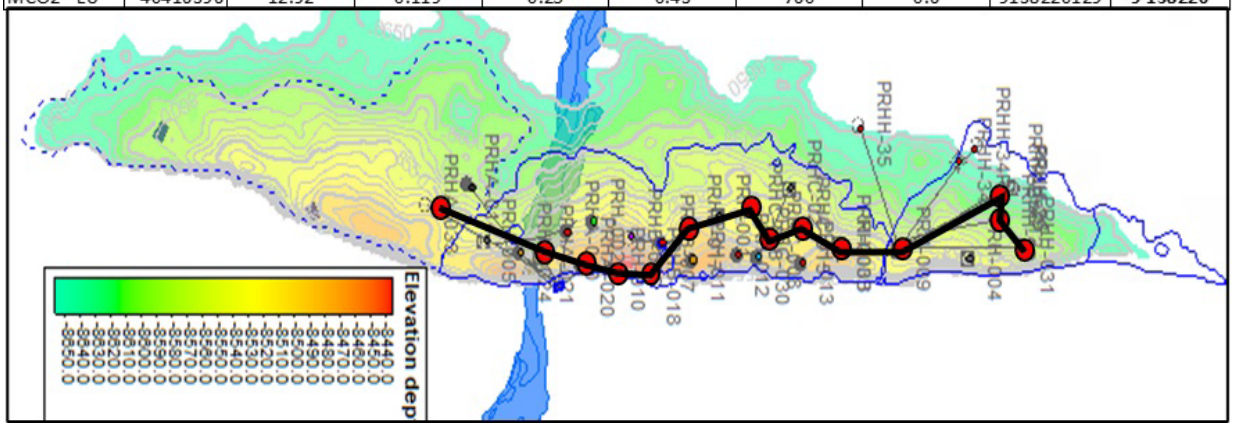

Figure 18. Excel spreadsheet with variables of equation and result and Lower U depth structure map clipped on 4-way structural closure.

4.12. Geomechanical risks

When stress magnitudes exceed the strength of the rock, the reservoir may fail. There is the possibility of re-activating faults when the maximum sustainable pressure is exceeded, this phenomenon can create new flow paths through which CO_2 can leak (Song et al., 2023).

5. Conclusions

• The Lower U reservoir exhibits continuous presence across the PRH field. While the net pay and lateral continuity decrease from north to south, the reservoir maintains a generally favorable overall continuity

• Petrographic analysis revealed quartz arenites and calcareous quartz arenites. The mineralogical composition is primarily composed of monocrystalline quartz.

• The dominant diagenetic process is mechanical compaction, while the chemical processes involve primary siliceous cementation and significant secondary calcareous cementation. Mineralogically, the samples exhibit a high quartz content of 84%, 11% kaolinite, and a low content of feldspars (5 %).

• Porosity is influenced by the secondary growth of quartz grains, resulting in absolute and effective porosity ranging from 3 to 15 %. This range aligns with the recommended criteria for CO_2 injection (Ø≥10%). Permeability varies between 42 to 637 mD, and the average wellbore skin factor is 4.5. Overall, the reservoir exhibits favorable fluid storage characteristics.

• The top seal of the Lower “U” reservoir consists of Limestone “A,” Limestone “M2,” and Limestone “M1” with shale intercalations, while the base is primarily composed of Limestone “B.” These formations collectively create an effective sealing system for the Lower “U” reservoir.

• The trajectory of injection wells, aimed at stabilizing LU and avoiding premature microfractures during CO_2 injection, is oriented at an azimuth approximately between 0º-90º and 190º-270º.

• Central area of the PRH field is the best candidate for CO_2 injection in the Lower “U” reservoir due to the lower reservoir pressure, water salinity and temperature. These characteristics allow injected CO_2 to stay in a supercritical phase. The theoretical storage volume for the Lower “U” reservoir in the PRH field is 9.13 million tons of CO_2.

References

Ayala, D., & Andrade, M. (2017). Factibilidad analítica de la aplicación de la recuperación mejorada de petróleo, caso de estudio Ecuador. *Fuentes, El reventón energético*, *15*(2), 19–30. https://doi.org/10.18273/revfue.v15n2-2017002

Ayala, D., Bastidas, A., Loaiza, M., & Ayala, S. (2018). Análisis litológico para incremento de la tasa de perforación en la cuenca oriente Ecuador. *Fuentes, El reventón energético*, *17*(1), 83–94. https://doi.org/10.18273/revfue.v17n1-2019008

Bachu, S. (2000). Sequestration of CO_2 in Geological Media: Criteria and Approach for Site Selection in Response to Climate Change. *Energy Conversion Management, 41*(9), 953-970. https://doi.org/10.1016/S0196-8904(99)00149-1

Bachu, S., Bonijoly, D., Bradshaw, J., Burruss, R., Holloway, S., Christensen, N., & Mathaissen, O. (2007). CO2 Storage Capacity Estimation: Methodology and Gaps. *International Journal of Greenhouse Gas Control, 1*(4), 430-443. https://doi.org/10.1016/S1750-5836(07)00086-2

Bady, P., Rivadeneira, M., & Barragan, R. (2014). *La Cuenca Oriente: Geología y Petróleo.* (3ª ed.). IFEA, IRD, PETROAMAZONAS EP.

Baines, S., & Worden, R. (2004). The long-term fate of CO2 in the subsurface: natural analogues for CO2 storage. *Geological Society London Special Publications, 233*, 29-85. https://doi.org/10.1144/gsl.sp.2004.233.01.06

Castillo, O., & Ortega, A. (2016). *Propiedades Petrofísicas y Aplicación en un Pozo Petrolero al Noreste de la República Mexicana*. [Bachelor's thesis]. Universidad Nacional Autónoma de México.

Catzíz, A., & Tobón, J. (2016). Caracterización inicial de yacimientos petroleros con base en la información del primer pozo perforado (Descubridor) [Bachelor's thesis]. Universidad Nacional Autónoma de México.

Chadwick, A., Arts, R., Bernstone, C., Franz, M., Thibeau, S., & Zweigel, P. (2007). *Best Practice for the Storage of CO2 in Saline Aquifers - Observations and Guidelines from the SACS and CO2 Store Projects*. Nottingham: British Geological Survey.

Chong, S., & Santamarina, J. C. (2016). Soil Compressibility Models for a Wide Stress Range. *Journal of Geotechnical and Geoenvironmental Engineering, 142*(6), 06016003. https://doi.org/10.1061/(ASCE)GT.1943-5606.0001482

Christopoulou, M. A., Koutsovitis, P., Kostoglou, N., Paraskevopoulou, C., Sideridis, A., Petrounias, P., Rogkala. A., Stock, S. & Koukouzas, N. (2022). Evaluation of the CO2 Storage Capacity in Sandstone Formations from the Southeast Mesohellenic trough (Greece). *Energies*, *15*(10), 3491. https://doi.org/10.3390/en15103491

E.P. PETROECUADOR. (2022). *Conversión del pozo SCY-31 a Inyector- Recuperación Secundaria.* Quito: E.P. PETROECUADOR.

Endara, I. (2015). *Estudio Petrográfico y Diagenético PRH-8 , Arenisca LU*. PETROPRODUCCIÓN.

Espinoza, D. N., & Santamarina, J. C. (2017). CO2 breakthrough—Caprock sealing efficiency and integrity for carbon geological storage. *International Journal Of Greenhouse Gas Control*, *66*, 218-229. https://doi.org/10.1016/j.ijggc.2017.09.019

Estupiñan, J., Marfil, R., & Permanyer, J. (2006). Diagenesis and Sequence Stratigraphy of the "U" Sandstone From the Napo Formation, Oriente Basin, Ecuador. *Geogaceta, 40*, 283-288.

Estupiñan, J., Marfil, R., Scherer, M., & Penmayer, A. (2010). Reservoir Sandstones of the Cretaceous Napo Formation U and T Members in the Oriente Basin, Ecuador: Links Between Diagenesis and Sequence Stratigraphy. *Journal of Petroleum Geology, 33*(3), 221-245. https://doi.org/10.1111/j.1747-5457.2010.00475.x

Estupiñan, J., & Pacheco, J. (2019). Mineralogía por Difracción de Rayos X (DRX) de la Muestra de los Pozos PRH 8,22; Zona UI y TI. Quito: CIQ.

Galarza, C. (2013). Almacenamiento Geológico de CO_2: Una Solución para la mitigación del Cambio Climático. *Anales de Química de la RSEQs, 109*(1), 20–26

Guéguen, Y., & Palciauskas, V. (1994). *Introduction to the Physics of Rock.* New Jersey: Princenton University Press.

Hurtado, A. (2009). *Metodología para la Estimación Regional de la Capacidad de Almacenamiento de CO_2 en Formaciones Permeables Profundas y sus Insertidumbres.* [Doctoral thesis]. Universidad de León.

Kaldi, J., Daniel, R., Tenthorey, E., Michael, K., Schacht, U., Nicol, A., Underschultz, J., & Backe, G. (2013). Containment of CO2 in CCS: Role of Caprocks and Faults. *Energy Procedia*, *37*, 5403-5410. https://doi.org/10.1016/j.egypro.2013.06.458

Loor, K., & Ruiz, R. (2022). *Proyecto Piloto para Inyección de Agua de Formación en T Inferior - Pozo Parahuacu - 22D.* Quito: E.P. PETROECUADOR-RESERVORIOS.

Ma, S., & Morrow, N. (1996). Relationships Between Porosity and Permeability for Porous Rocks. Montpelier: International Symposium of the Society of Core Analysis.

Medina, G., Flores, B., Endara, I., & Toro, J. (2011). *Distribución de Tamaños de Poros en la Arenisca T Inferior Pozo PRH-22D.* Quito: PETROPRODUCCIÓN.

Ministerio de Energía y Minas. (2022). Balance Energético Nacional 2021- Ecuador (Vol. 1 St). Quito: IIGE.

Montenegro, J., Medina, G., & Lascano, M. (2015). *Estudio Sedimentologico de la Arenisca U Inferior del Pozo PRH-8, Estudio de 13 ft del Núcleo Corona.* Quito: PETROPRODUCCIÓN.

Nygaard, R., Gutierrez, M., Hoeg, K., & Bjorlykke, K. (2004). Influence of burial history on microstructure and compaction behaviour of Kimmeridge clay. *Petroleum Geoscience*, *10*(3), 259-270. https://doi.org/10.1144/1354-079303-591

Olson, J., Laubach, S., & Lander, R. (2009). Natural fracture characterization in tight gas sandstones: Integrating mechanics and diagenesis. *AAPG Bulletin, 93*(11), 1535–1549. https://doi.org/10.1306/08110909100

Raeini, A., Bijeljic, B., & Blunt, M. (2015). Modelling Capillary Trapping Using Finite-Volume Simulation of Two-Phase Flow Directly on Micro-CT Images. *Advances in Water Resources, 83*, 102-110. https://doi.org/10.1016/j.advwatres.2015.05.008

Ringrose, P. (2020). *How to store CO2 Underground: Insights from early-mover CCS Projects. Springer Briefs in Earth Sciences* (1St ed.). Cham, Switzerland: Springer. https://doi.org/10.1007/978-3-030-33113-9

Silva, B. (2011). *Evaluación de Tecnologías de Recuperación Mejorada no Térmicas en el Campo Cerro Negro* [Bachelor's thesis]. Universidad de Oriente.

Toala, G., & Coello, X. (2008). *Estudio al Microscopio Electrónico de Barrido de Muestras de Núcleos de Corona, Pozo PRH-8 FM. Napo Superior.* Quito: PETROPRODUCCIÓN.

YACIMIENTOS-CIGQ. (2005). *Análisis Convencionales de Núcleo de Corona-Pozo PRH-8, Arenisca U Inferior.* Quito, Ecuador: PETROPRODUCCIÓN.

Pi, Y., Liu, J., Liu, L., Guo, X., Li, C., & Li, Z. (2021). The Effect of Formation Water Salinity on the Minimum Miscibility Pressure of CO2-Crude Oil for Y Oilfield. *Frontiers In Earth Science*, *9*. https://doi.org/10.3389/feart.2021.711695

Song, Y., Jun, S., Na, Y., Kim, K., Jang, Y., & Wang, J. (2022). Geomechanical challenges during geological CO2 storage: A review. *Chemical Engineering Journal, 456*, 140968. https://doi.org/10.1016/j.cej.2022.140968

Wang, M., Yang, Z., Shui, C., Yu, Z., Wang, Z., & Cheng, Y. (2019). Diagenesis and its influence on reservoir quality and oil-water relative permeability: A case study in the Yanchang Formation Chang 8 tight sandstone oil reservoir, Ordos Basin, China. *Open Geosciences, 11*(1), 37-47. https://doi.org/10.1515/geo-2019-0004

Wilkinson, M., Haszeldine, R. S., Fallick, A. E., Odling, N., Stoker, S. J., & Gatliff, R. W. (2009). CO2-Mineral Reaction in a Natural Analogue for CO2 Storage--Implications for Modeling. *Journal Of Sedimentary Research, 79*(7), 486-494. https://doi.org/10.2110/jsr.2009.052

Zheng , Q., & Liu, Y. (2015). Diagenesis and Diagenetic Lithofacies of Tight Reservoir of Chang4+5 Member of Yanchang Formation in Zhenbei, Ordos Basin. *Acta Sedimentologica Sinica, 33*(5), 1000-1012. https://doi.org/10.14027/j.cnki.cjxb.2015.05.016